Calibration of Ultrasonic Testing for Faults Detection in Stone Masonry

M. Usai[*1], S. Carcangiu[1], and G. Concu[2]
[1] Department of Electric and Electronic Engineering, University of Cagliari,
[2] Department of Civil Engineering, Environmental and Architecture,
*Corresponding author: Piazza d'Armi, 09123 Cagliari, Italy, s.carcangiu@diee.unica.it

Abstract: Building assessment and monitoring is a complex matter which forms a fundamental step for the proper management of buildings rehabilitation. In the field of assessment methodologies, particular importance is given to Non-Destructive Testing Techniques (NDTs), which aspire to achieve the highest number of information about materials and structures without altering their condition. Among NDTs, Ultrasonic Testing (UT) exploits the transmission and reflection characteristics of mechanical waves with appropriate frequencies passing through the investigated item.
An experimental program has been started with the aim of exploiting UT potentiality in stone masonry faults detection. A trachyte stone wall with an inside cavity has been used to test this methodology. COMSOL Multiphysics® has been used for modeling in the frequency domain the propagation of ultrasonic signals through the stone masonry, aiming at calibrating the characteristics of signal propagation by using data obtained from the experimental tests.

Keywords: Non-Destructive Testing, Finite Element Method, Ultrasonic Testing, Signal Processing, Frequency analysis.

1. Introduction

Stone masonry buildings form an integral part of the historical building heritage in Europe and throughout the world. When dealing with preservation and restoration of this kind of structures, it is necessary to assess their serviceability and, if possible, their load carrying capacity. Assessment of such buildings can however be difficult as there is little knowledge or experience available on their design, and the evaluation of their real state shouldn't interfere with the condition and the functionality of the building, and should possibly involve limited costs. To provide confidence for the assessment result, reliable input parameters are required and effective inspection and measurement methods are necessary to establish or verify the input parameters. Thus, inspection and monitoring of structural conditions is becoming an essential part of proper management of buildings rehabilitation.
In the field of assessment methodologies, particular importance is given to developments of NDTs, including automated procedures and information technology for evaluating data and supporting decision making. Among NDTs, UT are based on the principle that the propagation of any wave is affected by the medium through which it travels. Thus, changes in measurable parameters associated with the passage of a wave through a material can be correlated with changes in physical properties of the material itself [1- 3].
Elastic waves propagate in different manner through solid materials and cavities, thus enabling fault detection.
Due to media dissipative effect, elastic waves are strongly attenuated, so it is important that the emission cone of the signal source is less divergent as possible. If d is the diameter of the emission source and λ is the wavelength of the wave, for $d >> \lambda$ the wave is emitted with a not very divergent cone. As λ is in inverse proportion to frequency f, it is understandable how high frequency signals enable waves to be highly directional [1].
In this paper, the potentiality of an approach to ultrasonic investigation involving the analysis in the frequency domains of several parameters associated with acoustic waves propagating through the material has been analysed.
COMSOL Multiphysics® has been used for modelling a masonry wall, already built and tested in laboratory, in order to calibrate the characteristics of signal propagation. The model has been solved in the frequency domain, in order to decrease the size of resolution matrices, the time processing and the computational errors. Two sub-models have been considered: one for the emission probe (2D axisymmetric) and another for the wall (3D). The two models have then been coupled to perform the acoustic propagation in the wall (modelled by the Acoustic module) of the signal generated by the probe (modelled by the piezoelectric device

module).
Model parameters calibration has been made by comparing the ultrasonic signals simulated by numerical model to those detected by the receiving probe in laboratory tests.

2. Experimental session

The UT has been carried out on a trachyte stone masonry with a cavity inside. The wall is 90 cm wide, 62 cm high and 38 cm thick, and it is made of trachyte blocks sized $20 \times 38 \times 12$ cm^3, settled as shown in Figures 1-2 and jointed with cement lime mortar. The block assigned to the central position of the wall was not settled, thus realizing a macro-cavity with the same size of the missing block (Fig. 2), and assumed as a known anomaly. Mortar joints have been assumed to be 1 cm thick, but since the wall was manually built by a builder, actual dimensions are not so precise.

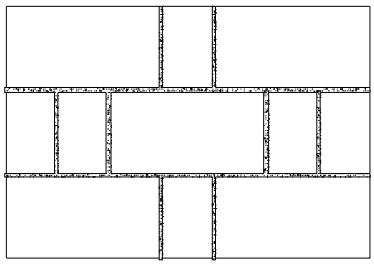

Figure 1. Front view of the wall**.**

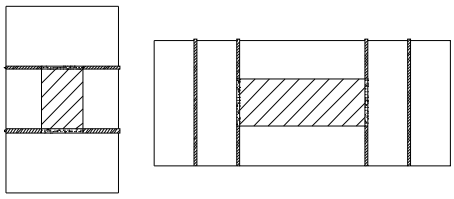

Figure 2. Vertical plane section: position of the cavity (left); Horizontal plane section intercepting the cavity (right)**.**

Trachyte specimens have been prepared and then tested following the Italian standards [9], obtaining a compressive strength of 40.5 MPa and a static elastic modulus of 6100 MPa.
The testing method is the Direct Transmission Technique (EN 14579 2004). In this method, the ultrasonic wave is transmitted by a transducer (emitter) through the test object and received by a second transducer (receiver) on the opposite side of the structure. Changes in received signal provide indications of variations in material properties.
In this case study, 308 emitters and 308 receivers have been arranged in a grid of 14×22 nodes in the opposite surfaces of the wall.
Ultrasonic measurements have been carried out using the ultrasonic test equipment Pundit Lab+, developed by Proceq.
The energizing signal is a square wave with high input voltage of 500 V (Fig. 3), which develops in a time interval of 9.24μs. The high intensity of this signal allowed signals on the other side of the wall to be detected even if strongly attenuated.

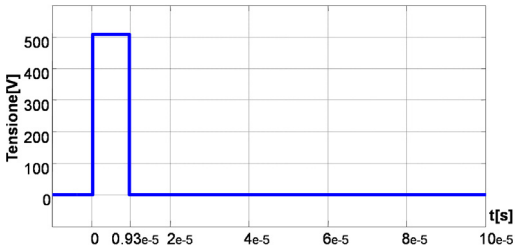

Figure 3. The energizing signal**.**

In the frequency range related to the harmonic components of the received signal, the average gain of the emission transducer is:

$$\frac{force}{voltage} = \frac{2}{10} = 0.2 \quad \left[\frac{N}{V}\right]$$

2.1 Wave Features Extraction and Analysis

During the experimental session a signal has been acquired for each point of the grid of receivers. From each node of the grid, several features in time domain and frequency domain have been extracted [4-8].
For each feature a distribution map in a vertical section of the wall has been performed, aiming at distinguishing variations in materials properties and macro-defects. In fact, signals have different patterns depending on the nature of the materials present along the travelled path.
It was possible to distinguish different types of signal paths, corresponding to different materials region in the wall (Fig. 4):

- trachyte path (pale blue),
- trachyte-mortar path (yellow),
- trachyte-mortar-air path (brown).

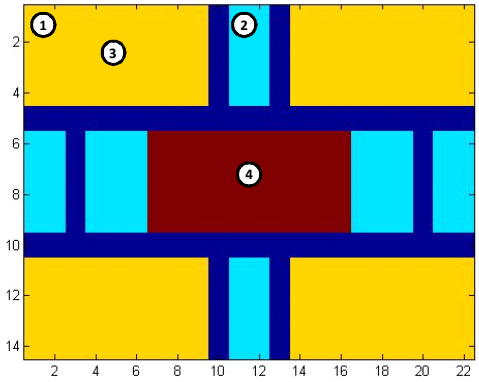

Figure 4. Map associated to the different materials of the wall.

As an example, Figures 5-8 show signals crossing the 4 paths shown in Fig. 4. It can be noted that these signals show different characteristics. In particular, it is worth noting that signals travelling close to the boundary of a materials region are different from those crossing the inner part of the same region.
Spectra of these 4 signals are shown in Figures 9-12. The harmonic content of the signals takes place around the resonant frequency of the transducer (54 KHz).

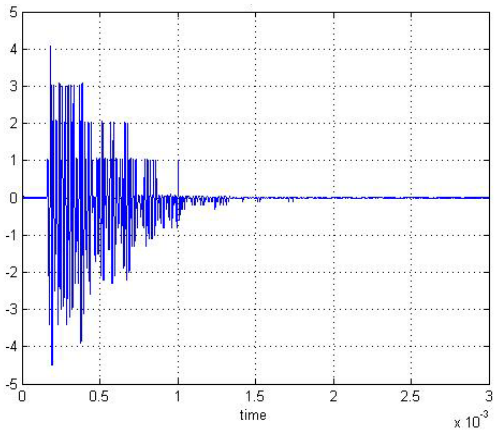

Figure 5. Signal acquired after travelling along path 1.

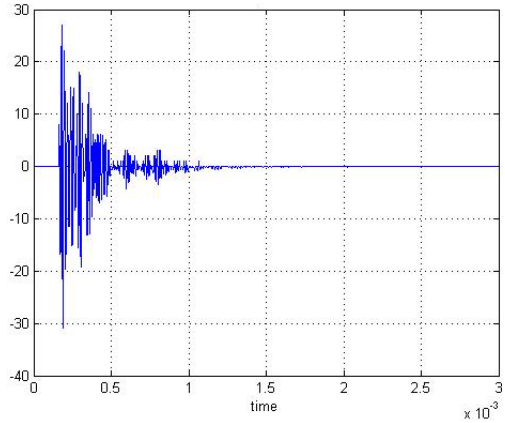

Figure 6. Signal acquired after travelling along path 2.

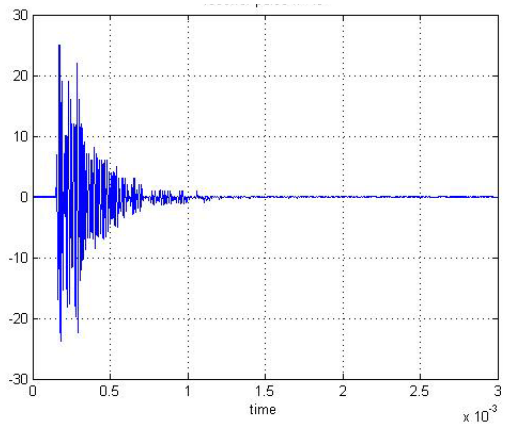

Figure 7. Signal acquired after travelling along path 3.

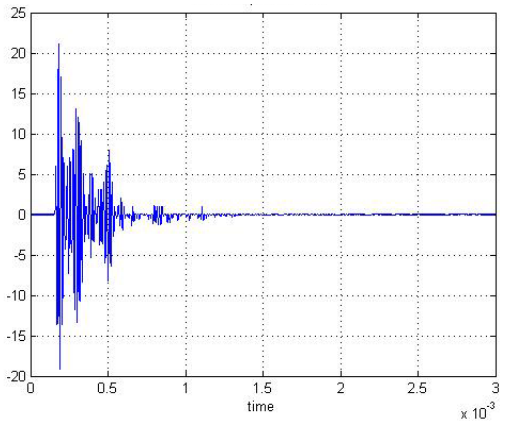

Figure 8. Signal acquired after travelling along path 4.

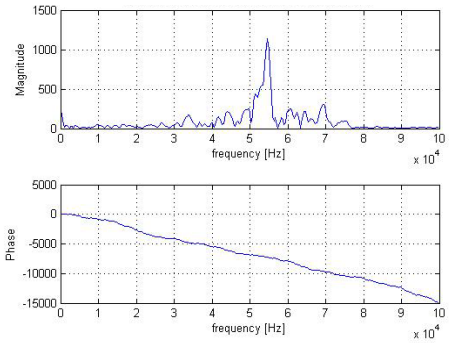

Figure 9. Spectrum of the measured signal-path 1.

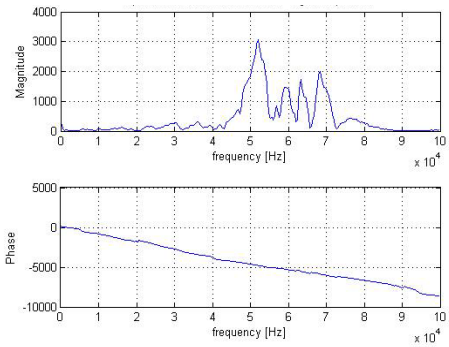

Figure 10. Spectrum of the measured signal- path 2.

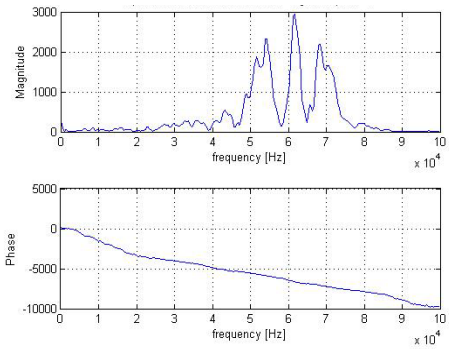

Figure 11. Spectrum of the measured signal-path 3.

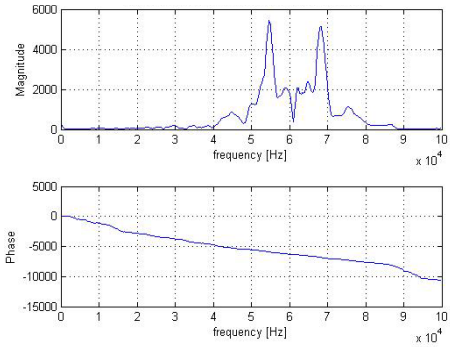

Figure 12. Spectrum of the measured signal-path 4.

3. Numerical model

The numerical analyses have been carried out using the *Acoustic-Solid Interaction* application model, belonging to the COMSOL Acoustics Module. In order to decrease the size of the resolution matrices, with significant reduction of processing time and computational errors, the frequency domain rather than the time domain has been chosen to solve the model. The sound field is described and solved by the pressure *p*.
Moreover, the *Acoustic-Piezoelectric Interaction* application mode, in the frequency domain, has been used for modeling the interface. To further reduce the computational time and the size of the problem, two sub-models have been considered: one for the emission transducer (2D axisymmetric) and another for the wall (3D).
The receiver transducer was not modeled in order to reduce errors due to the presence of a third sub-model and to reduce the problem dimension. This is possible because features maps can be performed by considering the acoustic pressure of received signals directly.
The two models have been coupled to perform the acoustic propagation in the wall (modeled by the Acoustic module) of the signal generated by the transducer (modeled by the piezoelectric device module) using the *Extrusion Model Couplings* option of COMSOL.
The acoustic pressure in the time domain *p(t)* is obtained as:

$$p(t) = \sum_{i=1}^{N} \left[p_{amp}(f) \cdot \cos\left(2\pi f \cdot t + p_{phase}(f)\right) \right]$$

$$f = \left[f_{\min} \div f_{\max} \right]$$

where $p_{amp}(f)$ e $p_{phase}(f)$ are respectively the module and the phase of the pressure *p* evaluated in the frequency domain and *N* is the number of components of the spectra in the frequency range.
The frequency spectrum is related to the type of energizing signal. For a square wave the Fourier spectrum presents the prevailing amplitudes in the field of frequency values:

$$-\frac{1}{\Delta} < f < \frac{1}{\Delta} \Rightarrow -108kHz < f < 108kHz$$

where Δ=9.24 μs, is the duration of the rectangular signal [10].

Nevertheless, as confirmed by the experimental data, the significant vibration modes effectively enabled have frequencies below 100 kHz and arrive at the maximum of 90 kHz.
For the entire model a mesh dense enough to accurately describe the propagating perturbation has been chosen. The length of the elements is equal to:

$$l_{\text{elem\_max}} = \frac{\lambda_{\min}}{20}$$

where λ_{min} is the minimum wavelength relative to the component of the transmitted signal with maximum frequency.

3.1. Acoustic Analysis of the 3D wall-model

A parametric analysis over a frequency range has been computed by the COMSOL simulator in order to obtain the frequency response of the 3D model shown in Fig. 13.

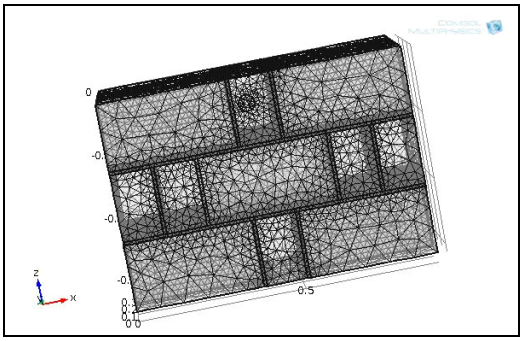

Figure 13. 3D wall-model with transducer positioned at point 2.

The acoustic pressure p_t in a medium is governed by the following equation that is an inhomogeneous Helmholtz equation:

$$\nabla \cdot \frac{1}{\rho_c}(\nabla p_t) - k_{eq}^2 \frac{p_t}{\rho_c} = Q$$

$$p_t = p + p_b$$

$$k_{eq} = \left(\frac{\omega}{c}\right)^2;\ k = \frac{\omega}{c} - j\alpha;\ \rho_c = \frac{\rho c^2}{c_c^2}$$

where ρ is the density of the material [kg/m^3], c is the speed of sound [m/s]; Q [1/s^2] is a monopole acoustic source, which is optional and has been neglected in this study.
In the presence of a background acoustic pressure wave p_b, the total acoustic pressure, p_t, is the sum of the pressure solved for, p, and the background pressure wave.
The attenuation coefficient α takes into account the damping of the acoustic waves that is mainly due to two factors: the first one is linked to the real absorption, which is a function of the frequency of the incident wave and the result of energy dissipation due to molecular friction; the second one is linked to scattering, which is a function of particle size that essentially make up the medium.
At the interface between the transducer and the wall, the boundary condition for the acoustics interface is that the pressure is equal to the normal acceleration of the solid domain:

$$\vec{n} \cdot \left(\frac{1}{\rho_0}(\nabla p)\right) = \vec{a}_n$$

where a_n is the normal acceleration. This drives the pressure in the wall domain.

3.2 Acoustic Analysis of the axisymmetric 2D transducer model

This model simulates a cylindrical PUNDIT transducer (Fig. 14) with a diameter of 0.050 m, a height equal to 0.035 m, and a protective metallic thickness of 4 mm. The transducer is made of Lead Zirconate Titanate PZT4-H, which is a common material in piezoelectric transducers.

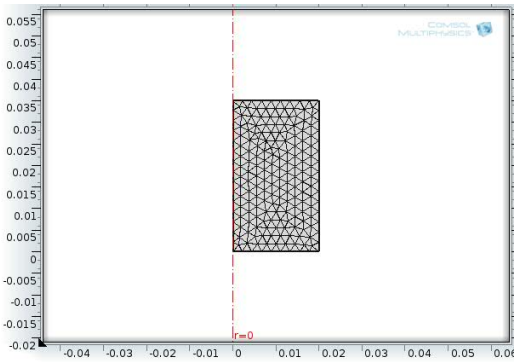

Figure 14. Axisymmetric-2D transducer model.

The element is rotationally symmetric, making it possible to set up the model in axially symmetric 2D.
The piezoelectric transducer can be used either to transform an electric current to an acoustic

pressure field or to produce an electric current from an acoustic field. The frequency is set to 54 kHz, which is the resonance frequency of this transducer.
An AC electric potential of 500 V is applied to the upper part of the transducer, while the bottom part is grounded.
The Piezoelectric Devices interface combines Solid Mechanics and Electrostatics for modeling of piezoelectric devices, for which some of the domains contain a piezoelectric material.
The mathematical formulation of this model is described by the equations:

$$-\rho\omega^2 u - \nabla\sigma = F_v e^{j\phi}$$

$$\nabla \cdot D = \rho_V$$

where F_v is deformation gradient, ρ_V is the volume charge density, u is the displacement, D is the electric displacement and σ is the stress-charge.

4. Numerical results

The acoustic analysis of the two coupled models in the frequency domain has led to obtain the spectrum of the signal in correspondence to the positions of the receiver transducer.
Signals spectrum has been evaluated in the range of frequency for which spectral amplitudes are significant for all the examined cases.
Simulated signals are shown in Figures 15-18. Simulated signals have duration of about 1.5 μs, according to the high speed of transmission of acoustic signals in the materials.

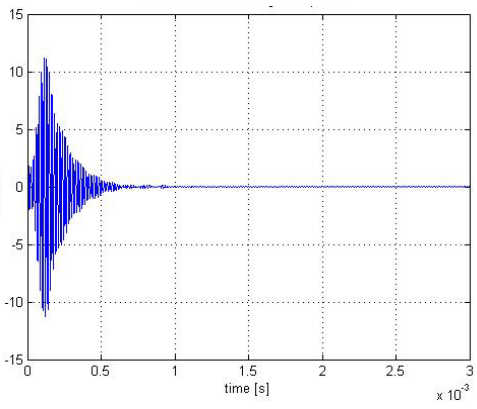

Figure 15. Simulated signal for path 1.

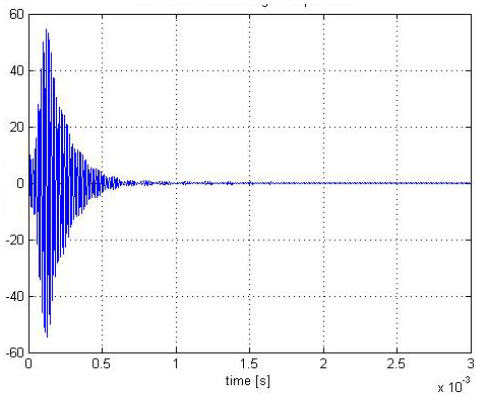

Figure 16. Simulated signal for path 2.

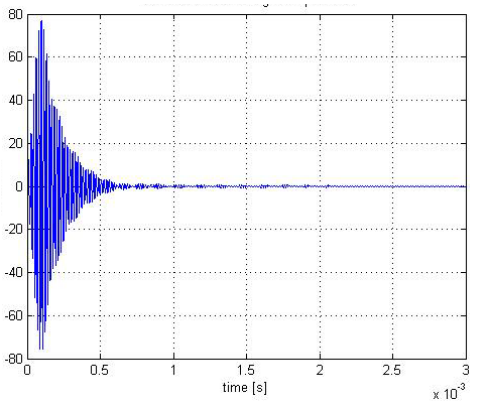

Figure 17. Simulated signal for path 3.

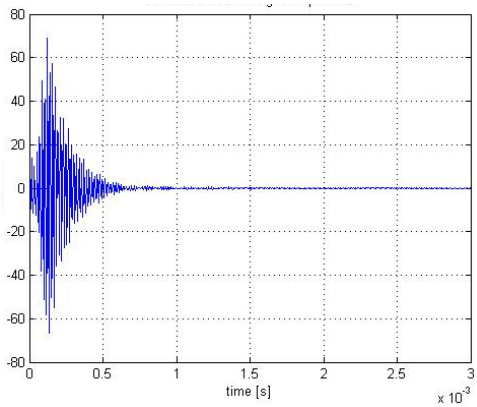

Figure 18. Simulated signal for path 4.

The transition time is very small even when the signal is applied to air regions, in which the signal covers a longer path along the boundary of this region. Signals amplitudes are different depending on the paths. The maximum amplitude occurs in the trachyte path (point 2) while the lower amplitude is in correspondence

of the trachyte-mortar-air path (point 4).
The amplitude decreases in the trachyte-mortar path where there are two interface involving reflections and attenuation (point 3). Finally, for paths crossing the same region (as points 1 and 2) there is a greater reduction in amplitude in correspondence of the points nearest to the interfaces and to the edges, indeed they are more exposed to the reflections of the transverse or shear waves and in general to all edge effects.
Furthermore, spectral analysis (Figures 19-22) shows that the harmonic content is strongly linked to the type of location and the proximity of this to interfaces and edges.
As can be noted, simulated signals show a performance in good agreement with experimental signals. Amplitudes in the time domain are scaled to the average gain of the emission transducer, while spectral bandwidths are shifted to higher values.

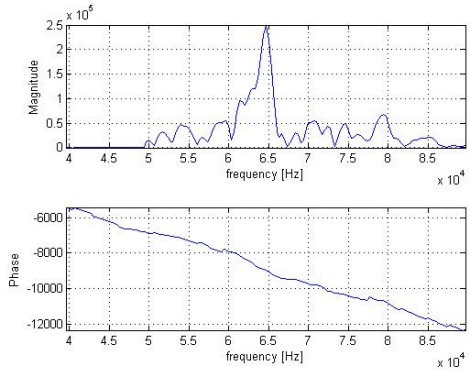

Figure 19. Spectrum of simulated signal path 1.

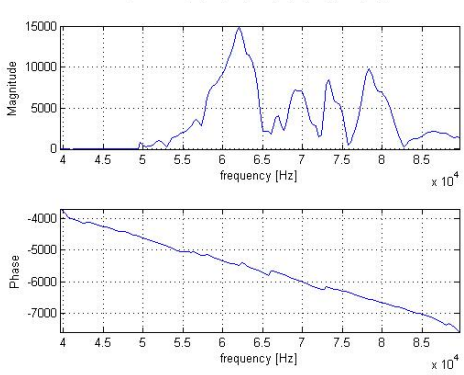

Figure 20. Spectrum of simulated signal path 2.

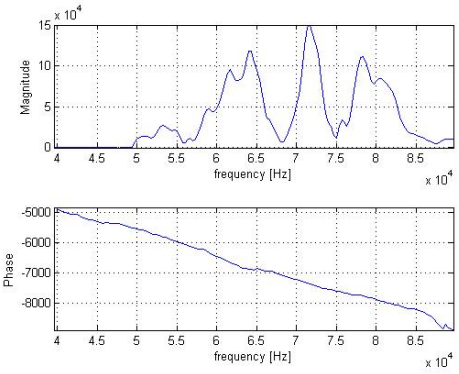

Figure 21. Spectrum of simulated signal path 3.

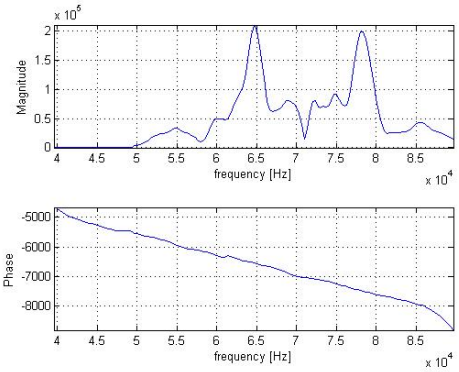

Figure 22. Spectrum of simulated signal path 4.

Similarly to what is found for the measured signals, also the simulated signals present different performances for the different types of paths, both in time domain and the frequency domain and this allows to post-process them to map the macro defects.

5. Conclusions

The purpose of this work was to create a model of a trachyte wall, built and tested in the laboratory, in order to simulate the ultrasonic signal propagation and thus be able to perform parametric studies freed from the experimental sessions. Model calibration has been archived by comparison of a significant sample of simulated signal to the correspondent signals obtained from the experimental sessions.
Results show that the implemented COMSOL model is suitable to effectively simulate the ultrasonic signals transmission to the stone wall.
The simulated signals can be used to obtain, through post-processing analysis, maps for detecting the presence of macro defects.

6. References

1. J. Krautkramer, H. Krautkramer, *Ultrasonic testing of materials*, Springer Verlag, New York, (1990).
2. M. Camplani, B. Cannas, F. Cau, G. Concu, M. Usai, Acoustic NDT on building materials using Features extraction techniques, *ICCSA 2008, Part II, Springer Lecture Notes in Computer Science* 5073, pp. 582–595, (2008).
3. M Berke., *Non-destructive material testing with ultrasonics*. Introduction to the basic principles. e-NDT5(2000).
4. Y.L Hinton. Problems associated with statistical patter recognition of acoustic emission signals in a compact tension fatigue specimen. *National Aeronautics and Space Administration*. NASA/TP-1999-209351 ARL-TR-1691(1999).
5. H.E. Katz, Acousto-Ultrasonics to Asses Material and Structural Properties. *National Aeronautics and Space Administration. NASA* /CR-2002-211881(2002.).
6. M.M. Reda Taha et al. Wavelet Transform for Structural Health Monitoring: a compendium of uses and features. *Structural Health Monitoring* 5: 267-295(2006).
7. D.V. Perov et al., Interaction of pulse ultrasonic signals with reflectors of different types. *Russian Journal of Nondestructive Testing* 43 (6): 369-377 (2007).
8. D.V. Perov & A.B. Rinkevich,Acoustic pulse signal diffraction from different reflectors in an elastic medium. *Insight* 50 (4): 216-217 (2008.).
9. EN 14579. 2004. Natural stone test methods – Determination of sound speed propagation.
10. B. Leland Jackson, *Digital Filters and Signal Processing* 3ed., Kluwer Academic Publishers 0-7923-9559-X

7. Acknowledgements

This work is supported by the operating program of Regione Sardegna (European Social Fund 2007–2013), L.R.7/2007, "Promotion of scientific research and technological innovation in Sardinia".